BIOCHEMISTRY
including biophysical chemistry & molecular biology

Article

pubs.acs.org/biochemistry

Control Activity of Yeast Geranylgeranyl Diphosphate Synthase from Dimer Interface through H-Bonds and Hydrophobic Interaction

Chih-Kang Chang, Kuo-Hsun Teng, Sheng-Wei Lin, Tao-Hsin Chang, and Po-Huang Liang*

Institute of Biological Chemistry, Academia Sinica, Taipei 11529, Taiwan

Supporting Information

ABSTRACT: Previously we showed that yeast geranylgeranyl diphosphate synthase (GGPPS) becomes an inactive monomer when the first N-terminal helix involved in dimerization is deleted. This raises questions regarding why dimerization is required for GGPPS activity and which amino acids in the dimer interface are essential for dimerization-mediated activity. According to the GGPPS crystal structure, three amino acids (N101, N104, and Y105) located in the helix F of one subunit are near the active site of the other subunit. As presented here, when these residues were replaced individually with Ala caused insignificant activity changes, N101A/Y105A and N101A/N104A but not N104A/Y105A showed remarkably decreased k_{cat} values (200−250-fold). The triple mutant N101A/N104A/Y105A displayed no detectable activity, although dimer was retained in these mutants. Because N101 and Y105 form H-bonds with H139 and R140 in the other subunit, respectively, we generated H139A/R140A double mutant and found it was inactive and became monomeric. Therefore, the multiple mutations apparently influence the integrity of the catalytic site due to the missing H-bonding network. Moreover, Met111, also on the highly conserved helix F, was necessary for dimer formation and enzyme activity. When Met111 was replaced with Glu, the negative-charged repulsion converted half of the dimer into a monomer. In conclusion, the H-bonds mainly through N101 for maintaining substrate binding stability and the hydrophobic interaction of M111 in dimer interface are essential for activity of yeast GGPPS.

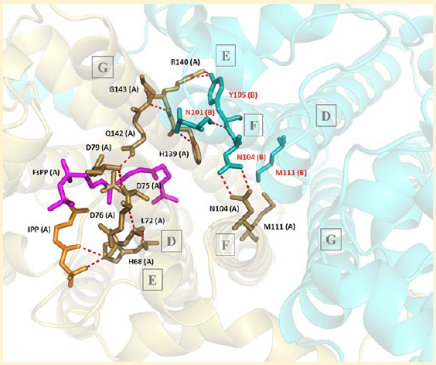

Geranylgeranyl diphosphate synthase (GGPPS) catalyzes the head-to-tail condensation of C_{15} farnesyl diphosphate (FPP) with C_5 isopentenyl diphosphate (IPP) to form C_{20} geranylgeranyl diphosphate (GGPP) product.[1−3] GGPP is the precursor of a variety of natural isoprenoid compounds including chlorophylls, α-tocepherol, longer prenyl diphosphates used in quinine biosynthesis, ent-kaurene, taxadiene, phytoene, and carotenoids.[4−8] Moreover, GGPP and FPP are ligands for protein prenylation, an essential posttranslational modification for anchoring signaling proteins such as Ras, Rho, Rab, and Rac onto cellular membranes.[9] Thus, GGPPS and FPP synthase (FPPS) that catalyze FPP formation through condensation of C_{10} geranyl diphosphate with IPP have been used as drug targets for developing therapy against cancer, osteoporosis, Paget's disease, hypercalcemia, and infectious diseases.[10]

GGPPS belongs to the *trans*-prenyltransferase family that catalyze IPP condensation reactions with allylic substrate (e.g., FPP) to form *trans*-double bonds, leading to different chain-length products. Members of this family synthesize the final products of C_{15} (FPPS), C_{20} (GGPPS), C_{30} [hexaprenyl diphosphate synthase (HexPPS)], C_{40} [octaprenyl diphosphate synthase (OPPS)], and up to C_{50} (decaprenyl diphosphate synthase); share sequence homology; and possess similar 3-D structures composed of fifteen α-helices connected by loops.[11−18] However, the dimeric GGPPS from *Saccharomyces cerevisiae* shows a unique positioning of its first N-terminal helix, which protrudes into and binds the opposite subunit.[16] Deletion of this helix [Δ(1−9) mutant] or simple removal of L8/ and I9 side chains (L8G/I9G double mutant) in this helix resulted in formation of monomeric GGPPS as determined by size exclusion chromatography and analytic ultracentrifugation, with loss of enzyme activity.[19]

There are growing numbers of examples in which dimerization is required for enzyme activity. The strategy of blocking active dimer formation has been used for drug development. In some cases, it is easy to understand why dimerization is required for enzymatic activity. For example, the protease of human immuno-deficiency virus (HIV) has an active site jointly formed by two monomers, each of which provides a catalytic Asp residue.[20] However, the answer is not obvious for GGPPS, where two active sites (one in each monomer) are separated. From the 3-D crystal structures of the yeast GGPPS,[16] three residues from chain B, N101(B), N104(B), and Y105(B), in the dimer interface formed by the highly conserved helix F are relatively closer to the active site of chain A and vice versa (Figure 1). These B-chain residues form hydrogen bonds with the A-chain residues, H139(A), N104(A), and R140(A), respectively, which may play roles in forming the functional active site. To address the roles of N101, N104, Y105, H139, and R140 in dimerization and enzyme activity, we created mutant GGPPS enzymes with single, double, and triple mutations to Ala on these amino acids.

Received: February 1, 2013
Revised: March 22, 2013
Published: March 27, 2013

   dx.doi.org/10.1021/bi4001276 | *Biochemistry* 2013, 52, 2783−2792

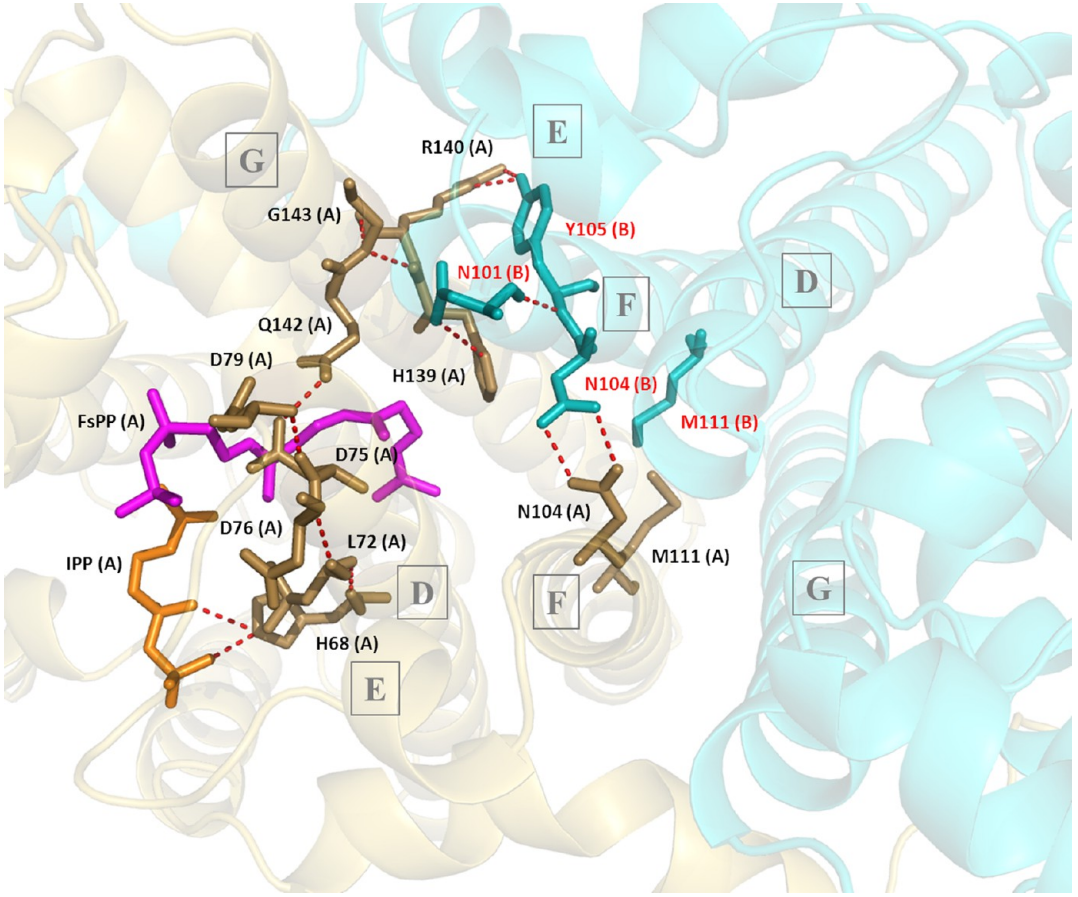

Figure 1. Crystal structure of yeast GGPPS showing N101, N104, Y105, and M111 in the central dimer interface. The carbon skeletons of N101(B), N104(B), Y105(B), and M111(B) are shown in cyan. The amino acids in monomer A, which are directly or indirectly connected to these amino acids, are displayed in brown. Hydrogen bonds are shown in red. Monomer A is shown in light brown, and monomer B is shown in light cyan. The substrate analog FsPP and the substrate IPP are shown in violet and orange, respectively.

On the basis of structural comparison of the yeast GGPPS with other *trans*-prenyltransferases (Figure 2), each subunit of yeast GGPPS uses a nonpolar residue of Met111 on F-helix to stack with Met111 from the other subunit. However, for human GGPPS, *Thermos thermophilus* GGPPS, and *Pyrococcus horikoshii* Ot3 GGPPS, aromatic amino acids for symmetric $\pi-\pi$ hydrophobic interaction are used. The crossing stacking interaction between Trp136 from monomer A and Pro114 from monomer B seems to be used in *Sulfolobus solfataricus* HexPPS.[12−15] Here, we also evaluated the role of M111 in dimerization of yeast GGPPS. Finally, a model for rationalizing why dimer is required for yeast GGPPS activity is proposed on the basis of our studies.

EXPERIMENTAL PROCEDURES

Materials. *PfuTurbo*, a plasmid miniprep kit, a DNAgel extraction kit, and Ni-NTA resin were purchased from Qiagen. A protein expression kit (including pET32Xa/LIC vector and JM109 and BL21 competent cells) was obtained from Novagen. A QuickChange site-directed mutagenesis kit was obtained from Stratagene. Radiolabeled [^{14}C]IPP (55 mCi/mmol) was purchased from Amersham Pharmacia Biotech. Nonlabeled FPP and IPP were obtained from Sigma. All commercial buffers and reagents were of the highest grade.

Site-Directed Mutagenesis of GGPPS. GGPPS mutant genes were prepared by using the QuickChange site-directed mutagenesis kit on the wild-type *S. cerevisiae* GGPPS-encoding gene[16,19] and ligated into pET32Xa/LIC vector. The mutagenic oligonucleotides used for PCR were 5′-ctcacttaatcttcggtgtaccctccactataGCGaccgcaaattatatgtatt-3′ for N101A, 5′-gtaccctccactataaacaccgcaGCGtatatgtatttcagagccatgcaa-3′ for N104A, 5′-accctccactataaacaccgcaaatGCGatgtatttcagagccatgcaac-3′ for Y105A, 5′-ggtgtaccctccactatagcgaccgcaGCGGCGatgtatttcagagccatgcaacttgta-3′ for N104A/Y105A, 5′-tatatgtatttcagagccGCGcaacttgtatcgcagc-3′ for M111A, 5′-tatatgtatttcagagccGAAcaacttgtatcgcagc-3′ for M111E, 5′-tatatgtatttcagagccTTCcaacttgtatcgcagc-3′ for M111F, 5′- acgattttcaacgaagaattgatcaatctaGCTaggggacaaggcttg-3′ for H139A, and 5′-ttcaacgaagaattgatcaatctacatGCGggacaaggcttgg-3′ for R140A (the mutated nucleotides are underlined and shown in capital letters). Δ(1−9) was constructed in our previous studies.[19] The multiple-site mutants were constructed with combination of the above mutagenic primers.

Expression and Purification of the Mutant GGPPS. The wild-type and mutant GGPPS were expressed in *Escherichia coli* and purified using NiNTA chromatography as previously described.[16,19] The constructed mutant plasmids were used to transform *E. coli* JM109 competent cells and the transformed cells were streaked on a Luria−Bertanim agar plate containing 100 μg/mL ampicillin. Ampicillin-resistant colonies were selected from the agar plate and grown in 5 mL of LB culture containing 100 μg/mL ampicillin overnight at 37 °C. The correct constructs confirmed by sequencing the entire genes were transformed to *E. coli* BL21(*DE*3) for protein expression.

dx.doi.org/10.1021/bi4001276 | *Biochemistry* 2013, 52, 2783−2792

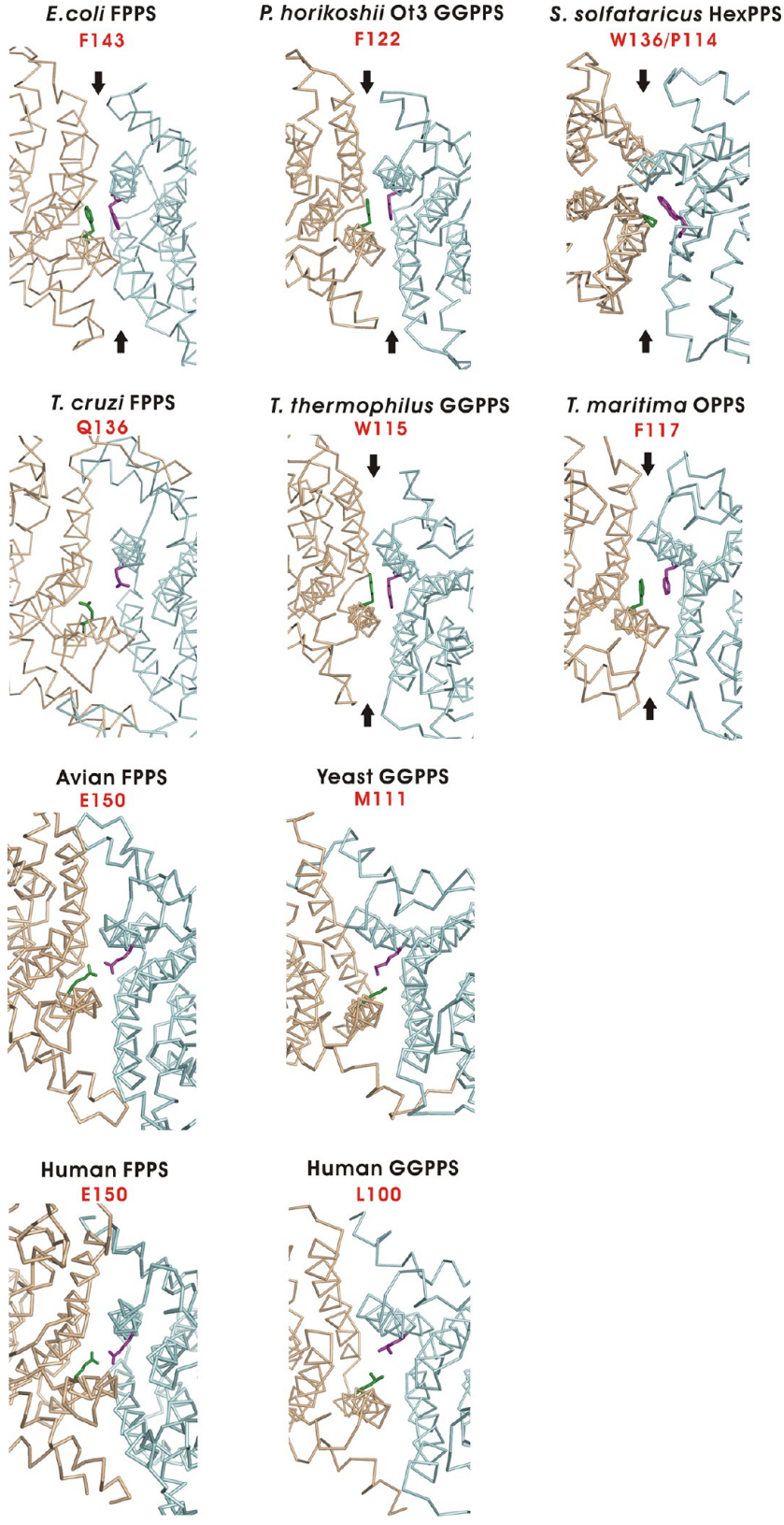

Figure 2. Critical amino acids in the center of the dimer interface as judged from the known structures of related *trans*-prenyltransferases. One subunit is shown in brown with its residue labeled in green, and the other subunit is shown in cyan with the interacting residue marked in purple. Except for the FPPS (*Trypanosoma cruzi*, avian, and human) and GGPPS (human and yeast), other *trans*-prenyltransferases use the aromatic residue for the π–π stacking interactions between two identical subunits for dimer formation. Black arrows indicate open area in the interface.

The 60 mL overnight culture of a single transformant was used to inoculate 6 L of fresh LB medium containing 100 μg/mL ampicillin. The cells were grown to A_{600} = 0.6 and induced with 1 mM IPTG at 16 °C. After 16 h of induction, cells were

dx.doi.org/10.1021/bi4001276 | *Biochemistry* 2013, 52, 2783−2792

Table 1. Kinetic Constants for Wild-Type and Mutant GGPPS

GGPPS	k_{cat} (s^{-1})	K_m(FPP) (μM)	K_m(IPP) (μM)	activity[a]
WT	3.7×10^{-2}	3.7 ± 0.7	1.7 ± 0.3	1
N101A	6.7×10^{-2}	6.3 ± 1.2	4.8 ± 0.9	1.81
N104A	1.1×10^{-1}	5.5 ± 1.5	5.5 ± 0.4	2.97
Y105A	6.0×10^{-2}	7.7 ± 1.8	2.6 ± 0.6	1.62
N101A/N104A	2.0×10^{-4}	15.3 ± 3.2	29.2 ± 7.9	0.005
N101A/Y105A	1.3×10^{-4}	6.1 ± 1.9	6.1 ± 1.8	0.004
N104A/Y105A	1.7×10^{-2}	46.7 ± 9.3	8.1 ± 2.5	0.46
N101A/N104A/Y105A	N.D.[b]	N.D.	N.D.	N.D.
M111A	4.0×10^{-2}	3.7 ± 0.7	2.5 ± 0.5	1.08
M111E	2.0×10^{-2}	9.0 ± 1.8	6.6 ± 1.2	0.54
M111F	3.6×10^{-2}	14.6 ± 4.3	11.3 ± 1.7	0.97
H139A[c]	4.2×10^{-2}	2.5 ± 1.1	5.1 ± 1.7	1.14
R140A	3.8×10^{-2}	8.9 ± 1.0	4.5 ± 1.0	1.03
H139A/R140A	N.D.[b]	N.D.	N.D.	N.D.

[a] k_{cat} values relative to that of the wild-type. [b] N.D., not detected. [c] Data taken from ref 16.

Table 2. Determination of Wild-Type and Mutant GGPPS Quaternary Structures by Size-Exclusion Column Chromatography

GGPPS	V_e (mL)	K_{av}	MW	composition
WT	158.87	0.26	82297	dimer
N101A	161.52	0.27	75948	dimer
N104A	159.66	0.26	80351	dimer
Y105A	162.05	0.27	74738	dimer
N101A/N104A	157.81	0.25	84984	dimer
N101A/Y105A	163.25	0.28	72069	dimer
N104A/Y105A	161.18	0.27	76734	dimer
N101A/N104A/Y105A	158.24	0.25	83883	dimer
M111A	155.07	0.24	92340	dimer
M111E	157.45/176.79	0.25/0.33	85915/47815	dimer/monomer
M111F	156.53	0.25	88077	dimer
H139A	160.35	0.26	78688	dimer
R140A	161.07	0.27	76990	dimer
H139A/R140A	178.95	0.34	44787	monomer
Δ(1−9)[a]	182.47	0.36	40255	monomer

[a] Δ(1−9) reported in ref 19 as a monomer was included here as a control.

harvested by centrifugation at 7000*g* for 15 min to collect the cell paste. Protein purification was conducted at 4 °C using the following procedure. The cell paste was suspended in 75 mL of lysis buffer containing 25 mM Tris−Cl, at pH 7.5, and 150 mM NaCl. Cell lysate was prepared with a French pressure cell press (AIM-AMINCO Spectronic Instruments) and centrifuged at 17000*g* to remove cell debris. The cell-free extract was then loaded onto the NiNTA column that had been equilibrated with lysis buffer containing 5 mM imidazole. The column was washed with 10 mM imidazole followed by 20 mM imidazole-containing buffer. His-tagged mutant GGPPS was eluted with 100 mM imidazole, dialyzed twice against 3 L of lysis buffer, subjected to the FXa protease digestion to remove the His-atg, and then reloaded into another NiNTA column to recover the untagged purified protein in flow through. SDS-PAGE analysis was used to confirm purity of the mutant GGPPS.

Enzyme Activity Assay. For enzymatic activity measurements, each 0.3 μM mutant GGPPS (N101A, N104A, Y105A, N101A/N104A, N101A/Y105A, N104A/Y105A, N101A/N104A/Y105A, M111A, M111E, M111F, R140A, and H139A/R140A) was used. The reaction was initiated in 200 μL solution containing 100 mM Hepes (pH 7.5), 20 μM FPP, 20 μM [^{14}C]IPP, 50 mM KCl, 0.5 mM $MgCl_2$, and 0.1% Triton X-100 at 25 °C. The total radioactivity used in the assay mixture was 0.4 μCi. The enzyme concentration used in all experiments was determined from its absorbance at 280 nm (ε = 20 340 M^{-1} cm^{-1}). To measure the initial rate, 40 μL portions of the reaction mixture were periodically withdrawn within 10% substrate depletion and then mixed with 10 mM EDTA to terminate the reactions. The radiolabeled product was then extracted with 1-butanol. The radioactivities in aqueous buffer ([^{14}C]IPP) and in butanol ([^{14}C]GGPP) were separately quantified by using a Beckmann LS6500 scintillation counter. The kinetic constants K_m and k_{cat} were obtained by fitting initial rate data with the Michaelis−Menten equation as previously described.[16,19]

Gel-Filtration Chromatography. For checking the molecular composition of mutant GGPPS, size exclusion chromatography using a HiLoad 26/60 Superdex 75 column calibrated with Blue Dextran 2000 was performed. Each mutant GGPPS was mixed with the molecular weight protein standards including Aldolase, Ovalbumin, Apomyoglobin, and Ribonuclease A (MW = 158 000, 44 000, 17 000, and 13 500 Da, respectively), loaded onto the size column and eluted with the buffer (25 mM Tris−HCl (pH 7.5) and 150 mM NaCl). The molecular weights of the mutant GGPPS were determined from

dx.doi.org/10.1021/bi4001276 | *Biochemistry* 2013, 52, 2783−2792

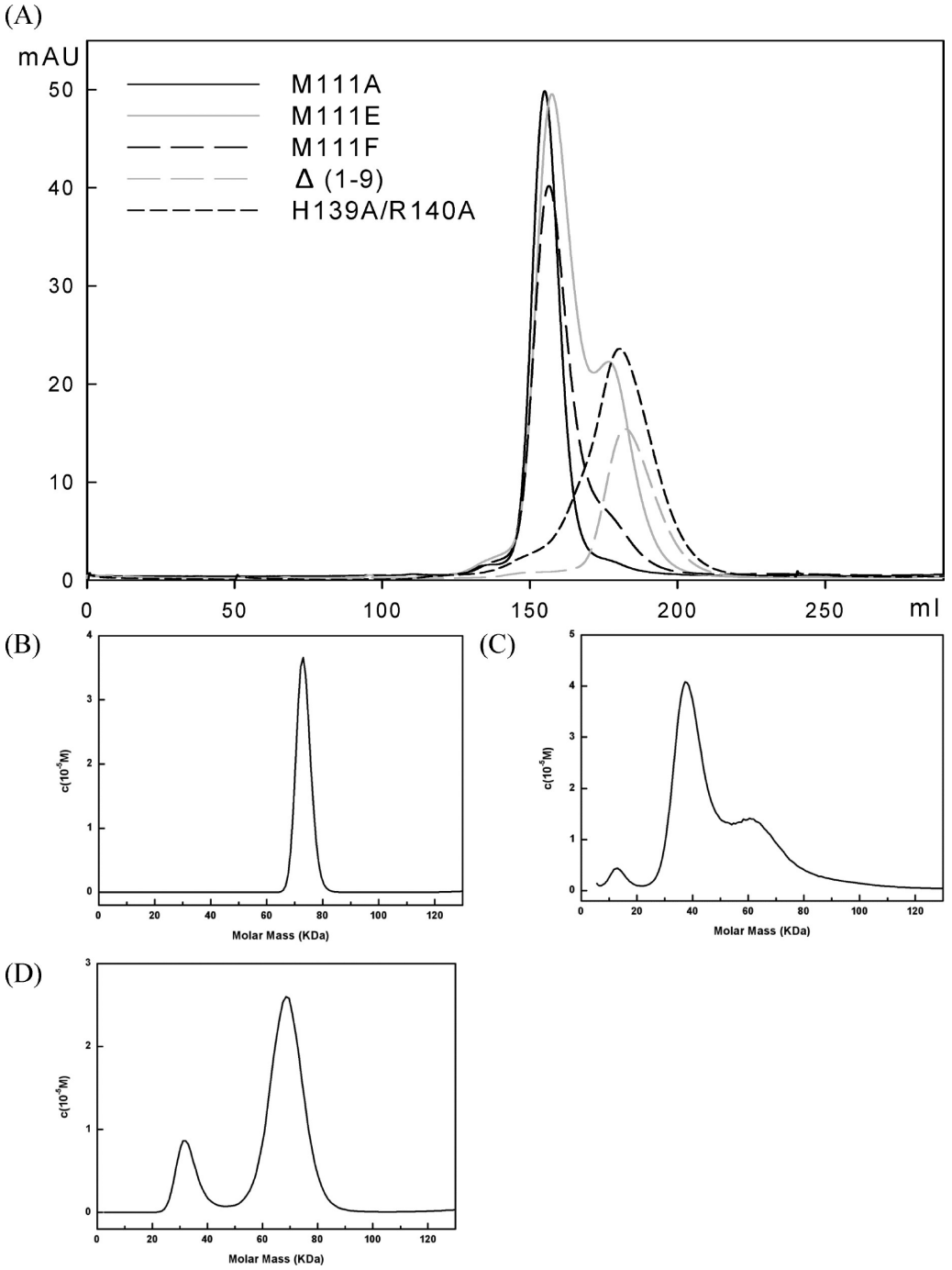

Figure 3. Elution profiles of size column chromatography for M111 mutants. (A) M111A is a dimer and M111E is a mixture of dimer (78 kDa) and monomer (39 kDa) according to the elution profiles. M111F adopts a dimer form, whereas Δ(1−9) used as a control here is a monomer as previously reported.[19] H139A/R140A is mostly monomeric with a small fraction of dimer. Moreover, the molar masses of wild-type and some mutant GGPPS were determined by AUC analysis. AUC profiles of (B) wild-type, (C) H139A/R140A, and (D) M111E mutants are shown.

a plot of K_{av} versus log MW of the protein molecular weight standards. K_{av} values were calculated from the equation $K_{av} = (V_e - V_o)/(V_t - V_o)$, where V_e is the elution volume of the mutant GGPPS, V_o is the elution volume of Blue Dextran 2000, and V_t is the total gel bed volume.

AUC Experiments. The molar masses of GGPPS (wild-type and mutants) were determined using analytical ultracentrifugation (AUC) as previously described.[19] The protein was diluted to 0.075 or 0.75 mg/mL for centrifugation. Sedimentation velocity studies were carried out with Beckman-Coulter XL-A analytical ultracentrifuge using an An 60Ti rotor. The experiments were performed at 20 °C and 40 000 rpm with a standard double-sector aluminum centerpiece. The experimental data were analyzed by Sedfit program version 12.1 (http://www.analyticalultracentrifugation.com). The Sednterp program (http://www.jphilo.mailway.com/) was used to calculate solvent densities and viscosities. After the ultracentrifugation experiments, the protein samples were visually checked for clarity and no indication of precipitation was found.

dx.doi.org/10.1021/bi4001276 | *Biochemistry* 2013, 52, 2783−2792

Circular Dichroism (CD) Experiments. CD measurements were made on a JASCO J-710 spectrometer in a 0.1 cm water-jacked cuvette. The 0.3 mg/mL wild-type and mutant GGPPS samples in 25 mM Tris (pH 7.5) buffer were subject to CD spectroscopic measurements and the CD spectra were obtained by scanning the samples from 200 to 250 nm collected at 20 nm/min with a 2 s response time; each spectral diagram was the final result averaged from five time scans. Their secondary structures were analyzed using the program SELCON2. The quantity of α-helix was estimated from the CD signal at 222 nm using the equation fH = $([\theta]_{222} - 3000)/(-36000 - 3000)$, where fH is the fractional helicity (in %) and $[\theta]_{222}$ is the mean molar residual elipticity at 222 nm (in deg·cm^2·dmol^{-1}).[21]

Structural Modeling of the Mutant Enzymes. The structures of N101A/N104A/Y105A and H139A/R140A mutant GGPPS were constructed with Discovery Studio software (Accelrys Discovery Studio 2.1; Accelrys Software Inc., San Diego, CA), using the "Build mutants" protocol from the "Protein modeling" module. The structure of the GGPPS in complex with FPP thiol analog FsPP and IPP (PDB access no. 2E8T) was used as a template for building the structural models.

RESULTS

Expression and Purification of Mutant GGPPS. Mutant yeast GGPPS were purified using NiNTA column chromatography and then by FXa treatment to remove the His-tag, followed by further purification using one more NiNTA to yield the tag-free proteins. Each purified mutant GGPPS showed a single band on the denaturing SDS-PAGE, indicating their great purity. Wild-type, N101A, N104A, Y105A, N101A/N104A, N101A/Y105A, N104A/Y105A, and N101A/N104A/Y105 are shown in Supplementary Figure 1A (Supporting Information). M111A, M111E, M111F, H139A, R140A, and H139A/R140A are shown in Supplementary Figure 1B (Supporting Information).

Activities and Quaternary Structures of the Mutant GGPPS Involving H-Bonds. To examine the impact of mutations on GGPPS activity, the kinetic constants of all mutant GGPPS were measured by isotope assays using FPP and radiolabeled [^{14}C]IPP as substrates. As summarized in Table 1, the purified mutants GGPPS showed k_{cat} values of 0.037, 0.067, 0.11, 0.06, 0.0002, 0.000 13, and 0.017 s^{-1} for WT, N101A, N104A, Y105A, N101A/N104A, N101A/Y105A, and N104A/Y105A, respectively. N101A, N104A, and Y105A single mutants did not show significantly changed activity. In contrast, the double mutants, N101A/N104A and N101A/Y105A, showed remarkably reduced k_{cat} values (0.005- and 0.004-fold of the wild-type activity, respectively), while N104A/Y105A showed no significantly reduced k_{cat} value (0.46-fold of the wild-type activity), indicating that N101 is the most important amino acid in the dimer interface for activity. More importantly, the activity of triple mutant N101A/N104A/Y105A was not detected (N.D.) (Table 1). However, on the basis of size chromatography, all of the mutants remained dimers (Table 2). This indicates that the mutations were not sufficient to disrupt dimerization but caused loss of activity due to the missing H-bonds from the side chains.

From Figure 1, the side chains of N101(B) and Y105(B) form H-bonds with the side chains of H139(A) and R140(A), respectively. Therefore, the N101A/Y105A mutant enzyme without these two H-bonds showed significantly impaired activity as mentioned above. We then constructed two single mutants, H139A and R140A, and found the mutant GGPPS did not lose enzyme activity (their k_{cat} values were 0.042 and 0.038 s^{-1}, respectively, as summarized in Table 1), consistent with the activities of N101A and Y105A. However, the activity of the double mutant H139A/R140A was not detected. Surprisingly, the double mutant became a monomer as a major species with minor contamination of dimer as revealed by size chromatography (Figure 3A) and AUC (Figure 3C), while the wild-type GGPPS is a dimer (Figure 3B). Although there were some dimeric protein molecules, H139A/R140A showed no detectable activity, indicating the residual dimer with these two mutations was inactive. This was confirmed later by CD measurement showing that H139A/R140 was not folded properly as the wild-type.

Function of M111 in Dimerization. To elucidate the possible function of the amino acid residue in the center of the dimer interface, Met111 was changed to Ala (M111A) to simply remove the hydrophobic side chain. Similar activity was observed (1.08-fold of the wild-type activity as shown in Table 1), and the mutant protein existed as a dimer (Table 2). In contrast, M111E, introduction of a negative charge residue of Glu in the interface resulted in a partial shift from dimer to

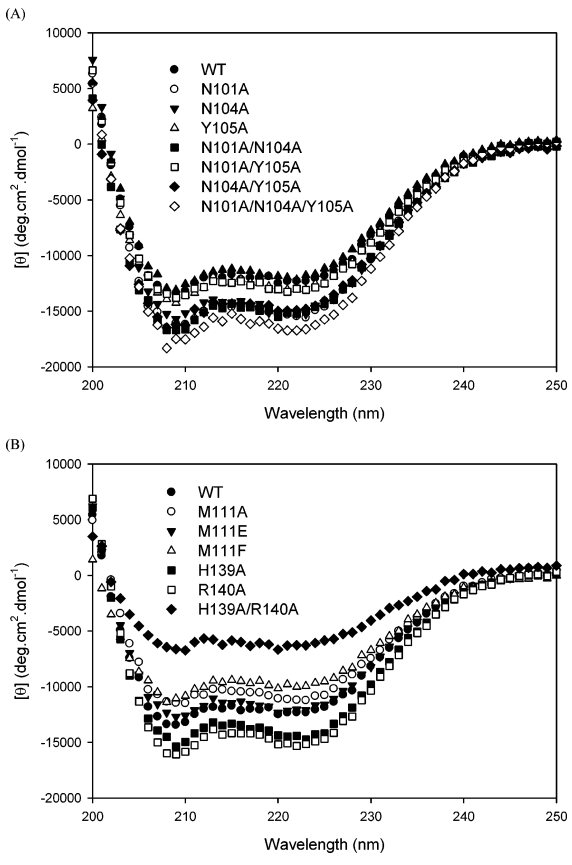

Figure 4. Analyses of the secondary structures of wild-type and mutant GGPPS using CD. CD spectra of the wild-type and a series of mutants on N101, N104, and Y105 are shown in (A); CD of the wild-type and a series of mutants on M111, H139, and R140 are shown in (B). The ellipticities of wild-type and mutant GGPPS were recorded from 200 to 250 nm, which reveal similar helix-rich secondary structures, consistent with the GGPPS crystal structure, except for the H139A/R140A double mutant, which is mainly a monomer.

dx.doi.org/10.1021/bi4001276 | Biochemistry 2013, 52, 2783−2792

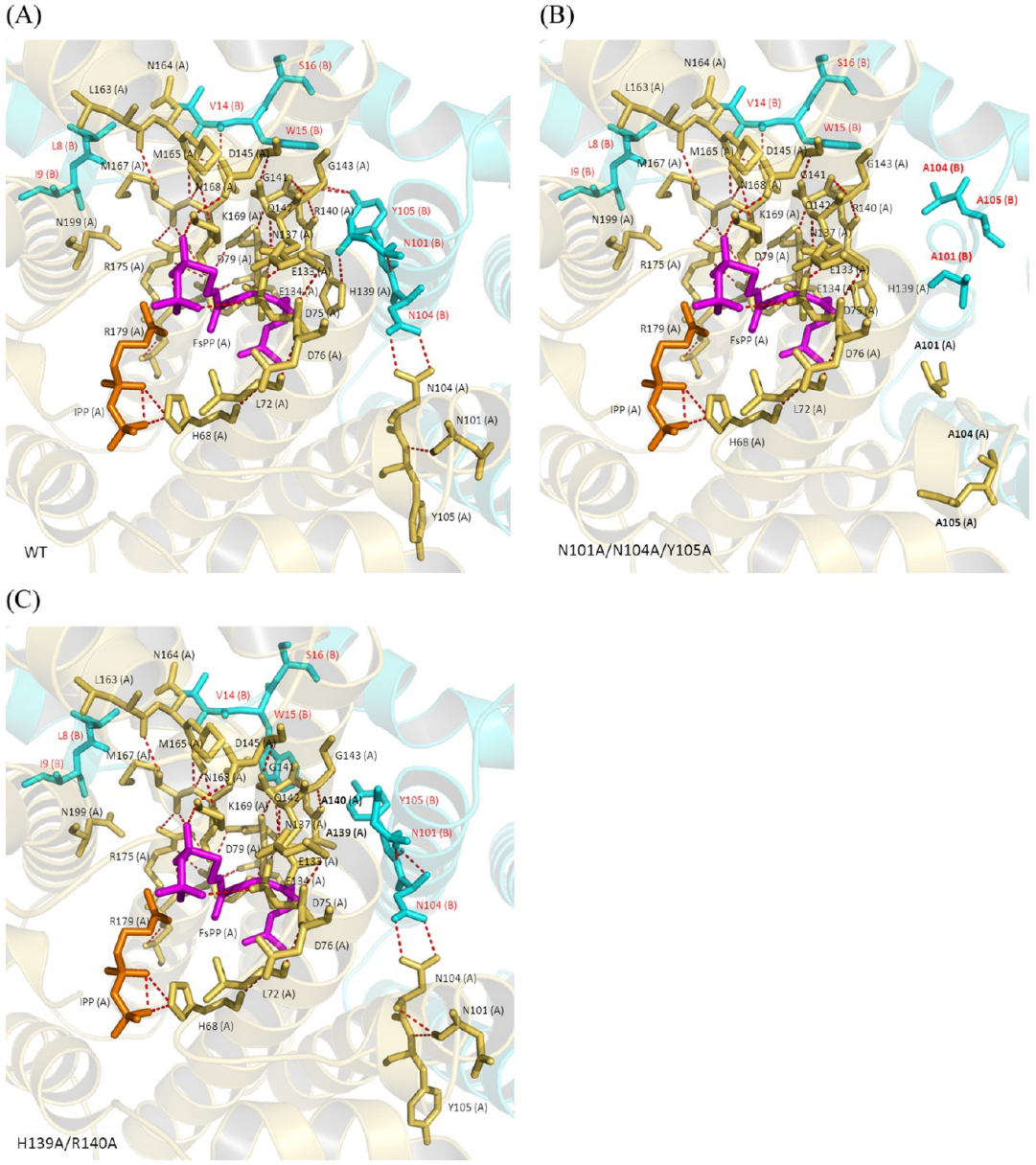

Figure 5. Structural modeling of N101A/N104A/Y105A and H139A/R140A displaying the lost H-bonds. The amino acids linking the dimer interface to the active site as well as FsPP and IPP are shown with the same color presentation used in Figure 1. The mutated amino acids are labeled in bold. Compared to the H-bond network of the wild-type shown in (A), 101A/N104A/Y105A in (B) lost the H-bonds due to mutations. H139A/R140A in (C) has additional loss of V14−N168, M165−N168, and E133−N137 H-bonds besides the lost H-bonds due to the mutated side chains. This additional H-bond loss in H139/R140 may impair N-terminal interaction, thereby resulting in monomer.

monomer as revealed by the size column chromatography (Figure 3A) with 0.54-fold of the wild-type catalytic activity (Table 1). Because the peaks of monomer and dimer were partially overlapping in the elution profile, it was impossible to accurately estimate the relative quantities of monomer versus dimer. Therefore, AUC measurements were used to reveal that 66.3% of the protein was retained as a dimer (Figure 3D), consistent with the remaining activity. As expected, the replacement of M111 with hydrophobic Phe in GGPPS maintained the dimeric form (Table 2), and the M111F activity was similar to that of the wild-type (Table 1). These data suggest hydrophobic interaction at this position is required for dimerization.

Secondary Structures of the Mutant GGPPS. To know whether the mutants with impaired activities were folded properly, their CD spectra were measured. The ellipticity of each sample containing 0.3 mg/mL protein in a buffer of 25 mM Tris (pH 7.5) and 150 mM NaCl at 25 °C was recorded from 200 to 250 nm. As shown in Figure 4A, the CD spectra of those GGPPS mutants (except the monomeric H139A/R140A) were similar to that of the wild-type, displaying α-helical secondary structures consistent with the reported 3-D structure, indicating their proper folding. To estimate the quantity of α-helix in GGPPS mutants, the fractional helicity (fH) was measured to be 0.47 (N101A), 0.47 (N104A), 0.41 (Y105A), 0.47 (N101A/N104A), 0.41 (N101A/Y105A), 0.46 (N104A/Y105A), and 0.51 (N101A/N104A/Y105A), similar to that (0.39) of the wild-type. While H139 and R140A also showed similar fH, 0.45 and 0.47, respectively, as compared to that of the wild-type, fH of H139A/R140A double mutant was

dx.doi.org/10.1021/bi4001276 | *Biochemistry* 2013, 52, 2783−2792

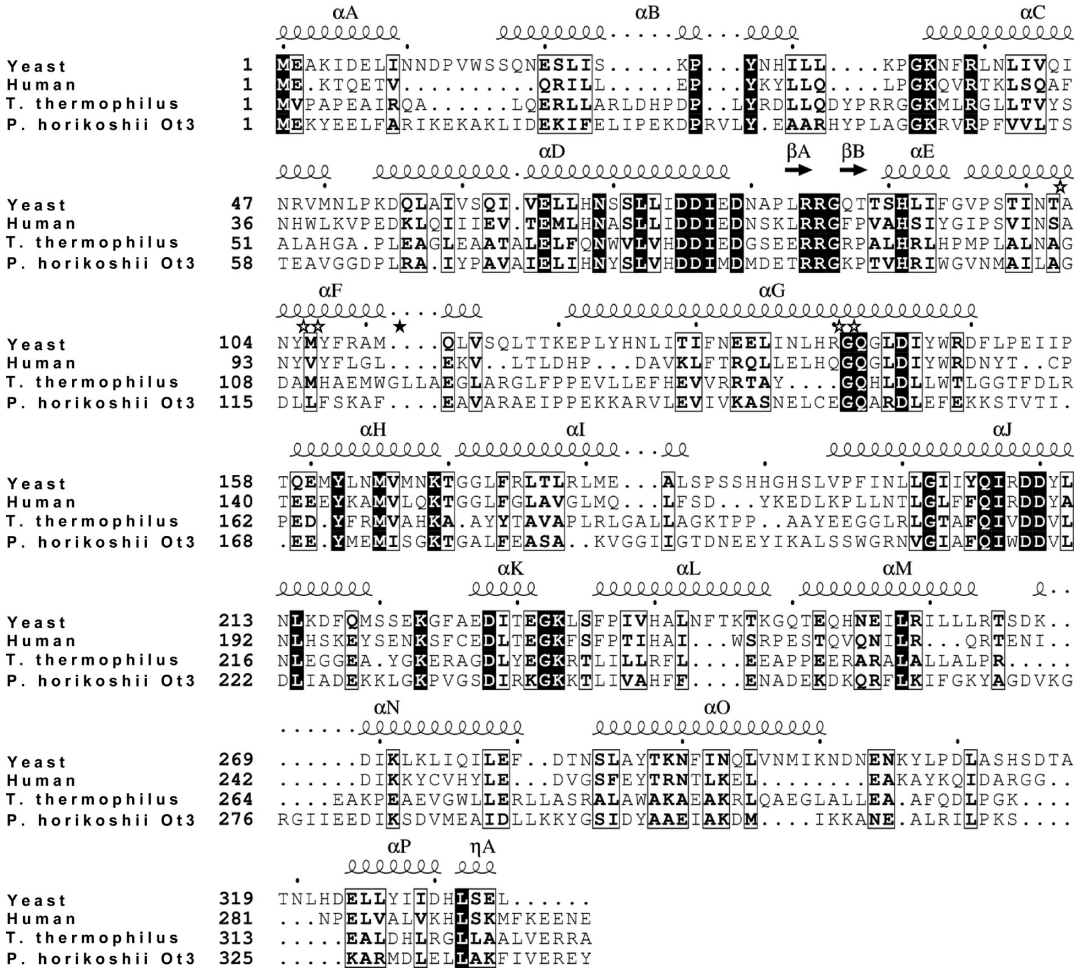

Figure 6. Alignment of amino acid sequences of GGPPS from *S. cerevisiae* (PDB accession no. 2DH4), human (PDB accession no. 2Q80), *T. thermophilus* (PDB accession no. 1WMW), and *P. horikoshii* Ot3 (PDB accession no. 1WYO). This figure is created by CLC Sequence Viewer 6 and ESPript 2.2 software. Identical and similar amino acid residues are shown in white with black background and bold, respectively. The regions of the 16 helices of *S. cerevisiae* GGPPS are indicated at the top. The open and filled stars indicate the amino acid residues mutated here for studying the H-bonding network and hydrophobic interaction, respectively.

significantly lower (0.24), indicating loss of the α-helical content. The conserved secondary structures were also observed for the M111A and M111F (Figure 4B). The same fH of 0.39 was observed for both M111A and M111F as the wild-type, but that for M111E, which contained monomeric structure, was slightly lower (fH = 0.36).

DISCUSSION

As revealed by the crystal structure of yeast GGPPS in complex with FsPP and IPP (Figure 5A), the carbonyl oxygen of the amide bond between H139(A) and R140(A) in chain A are H-bonded (2.78 Å) with the amide-bond nitrogen between G143(A) and the next amino acid Q142(A) that in turn is H-bonded (3 Å) to D75(A). D75 is within the first DDXXD motif, a conserved motif proven to be essential for catalysis of all *trans*-prenyltransferases by coordinating Mg^{2+} ions to bind with the diphosphate group of FPP and facilitate the farnesyl carbocation intermediate formation for nucleophilic attack by IPP.[22,23] D75 is also indirectly involved in the binding of the other substrate IPP by H-bonding with L72 and H68. The H-bonding network initiated by the interactions of N101(B)−H139(A) at a distance of 3.27 Å or Y105(B)−R140(A) at 3.24 and 3.16 Å are apparently important in maintaining the orientations of the substrates for condensation reaction. Therefore, N101A/Y105A showed remarkably lower enzyme activity, and H139A/R140A lost all the enzyme activity.

It is worth noting that H139A/R140A becomes a monomer while N101A/N104A/Y105A remains as a dimer, although both enzymes have lost activity. It is likely this is because H139 and R140 are not only H-bonding with the N101 and Y105 from the opposite subunit in the dimer interface but also interacting with the other amino acids within the same subunit. According to the structural modeling of these two mutant enzymes shown in parts B and C of Figure 5, N101A/N104A/Y105A has lost H-bonds due to the mutated side chains only, but H139A/R140 causes breakage of additional H-bonds, including V14−N168, M165−N168, and E133−N137 H-bonds. These H-bonds have been implicated in the H-bond network stabilizing dimerization by the first N-terminal helix.[19] Mutations of H139 and R140 to Ala thus result in the loss of H-bonds not only in the central intersubunit interface with N101 and Y105 from helix F but also in the N-terminus-mediated interactions stemming from L8 and I9 of helix A, thereby causing H139A/R140A to become a monomer. Therefore, the intersubunits' interactions provided by both N-terminus (helix A) and the central dimer interface (helix F) are important for maintaining activity of yeast GGPPS in a dimeric form.

dx.doi.org/10.1021/bi4001276 | *Biochemistry* 2013, 52, 2783−2792

However, one single mutation on N101A, Y105A, H139A, or R140A does not cause reduced activity (the less than 5-fold better activities of the mutants enzymes as compared to that of the wild-type probably due to structural flexibility are regarded insignificant). Apparently, the H-bonds through the interaction of N101 with H139 or Y105 with R140 can compensate each other to maintain the active conformation and thus the enzyme activity. However, compared to Y105, N101 is more important for keeping up the activity because the two double mutants N101A/N104A and N101A/Y105A (both containing N101A mutation) show remarkably reduced activities, whereas N104A/Y105A causes less impact on k_{cat}. From the sequence comparison of the homologous proteins (Figure 6), N101, N104, and Y105 are all conserved among the GGPPS from different species, suggesting their importance. From our mutagenesis data, N104, which forms H-bonds with N104 in the opposite subunit, seems less important than N101 and Y105. However, the triple mutant N101A/N104A/Y105A showed nondetectable enzyme activity, much worse than the two double mutants N101A/N104A and N101A/Y105A, suggesting N104 still plays a minor role in dimerization-mediated activity.

The residue of Met111 located in the center of the interface was also demonstrated here to be involved in dimerization. The repulsion caused by the negative charge residue of Glu at the position of M111 can lead to partial conversion of a dimer to a monomer. The sequence homology among the GGPPS enzymes (Figure 6) shows that the amino acids at this position are not conserved. Leu100 in the crystal structure of human GGPPS (Figure 2) that is a tetramer rather than a dimer,[17] may play a similar role to Met111 of the yeast GGPPS in enhancing its interface interaction. However, some short-chain *trans*-prenyltransferases such as FPPS (*T. cruzi*, avian, and human) and GGPPS (human and yeast) have nonhydrophobic residues at this position. In these cases, the enzymes seem to use the N-terminal helix to provide extra interaction for keeping dimerization, as judged from their crystal structures. On the other hand, the other *trans*-prenyltransferases that have tighter $\pi-\pi$ stacking interactions in their central interface seem to have their first helix outward without holding the opposite subunit.

Dimerization is required for activity of yeast GGPPS. In the previous study, we showed the first N-terminal helix (helix A) including the 9 amino acids to embrace the other monomer in yeast GGPPS is essential for dimer formation.[19] Two networks of interactions, one stemming from L8 and the other from I9, are disrupted when helix A is deleted or the side chains of L8 and I9 are removed, leading to a monomer.[19] The monomeric yeast GGPPS thus missing the H-bonds and hydrophobic interaction in the central dimer interface (helix F) as illustrated here will lose enzyme activity. The information obtained in this study enhances our understanding on the functions of amino acids in the dimer interface of yeast GGPPS and helps to answer the general question of how interactions between subunits are required for enzyme activity. Due to the sequence homology between the yeast and other GGPPS, the information may be also useful for developing inhibitors to disrupt the active human's or pathogens' GGPPS from the intersubunit interfaces, which are important drug targets.

■ ASSOCIATED CONTENT

Supporting Information

The SDS-PAGE gels of the purified mutant GGPPS are available free of charge via the Internet at http://pubs.acs.org.

■ AUTHOR INFORMATION

Corresponding Author

*E-mail: phliang@gate.sinica.edu.tw. Tel: +886-2-3366-4069. Fax: +886-2-2363-5038.

Funding

This work was supported by grants from Academia Sinica and National Science Council (grant number: 99-2113-M-001-014-MY3).

Notes

The authors declare no competing financial interest.

■ ACKNOWLEDGMENTS

We thank Academia Sinica's core facility for providing CD and AUC instruments.

■ ABBREVIATIONS

GGPPS, geranylgeranyl diphosphate synthase; FPP, farnesyl diphosphate; IPP, isopentenyl diphosphate; GGPP, geranylgeranyl diphosphate; FPPS, farnesyl diphosphate synthase; HexPPS, hexaprenyl diphosphate synthase; OPPS, octaprenyl diphosphate synthase; FsPP, farnesyl *S*-thiolodiphosphate

■ REFERENCES

(1) Sacchettini, J. C., and Poulter, C. D. (1997) Creating isoprenoid diversity. *Science 277*, 1788−1789.

(2) Ogura, K., and Koyama, T. (1998) Enzymatic aspects of isoprenoid chain elongation. *Chem. Rev. 98*, 1263−1276.

(3) Liang, P. H. (2009) Reaction kinetics, catalytic mechanisms, conformational changes, and inhibitor design for prenyltransferases. *Biochemistry 48*, 6562−6570.

(4) Rudiger, W., Benz, J., and Guthoff, C. (1980) Detection and partial characterization of activity of chlorophyll synthetase in etioplast membranes. *Eur. J. Biochem. 109*, 193−200.

(5) Jiang, Y., Proteau, P., Poulter, D., and Ferronovick, S. (1995) Bts1 encodes a geranylgeranyl diphosphate synthase in *Saccharomyces cerevisiae*. *J. Biol. Chem. 270*, 21793−21799.

(6) Olszewski, N., Sun, T. P., and Gubler, F. (2002) Gibberellin signaling: Biosynthesis, catabolism, and response pathways. *Plant Cell 14*, S61−S80.

(7) Dogbo, O., Laferriere, A., Dharlingue, A., and Camara, B. (1988) Carotenoid biosynthesis - Isolation and characterization of a bifunctional enzyme catalyzing the synthesis of phytoene. *Proc. Natl. Acad. Sci. U. S. A. 85*, 7054−7058.

(8) Kuzuguchi, T., Morita, Y., Sagami, I., Sagami, H., and Ogura, K. (1999) Human geranylgeranyl diphosphate synthase - cDNA cloning and expression. *J. Biol. Chem. 274*, 5888−5894.

(9) Clarke, S. (1992) Protein isoprenylation and methylation at carboxyl-terminal cysteine residues. *Annu. Rev. Biochem. 61*, 355−386.

(10) Guo, R. T., Cao, R., Liang, P. H., Ko, T. P., Chang, T. H., Hudock, M. P., Jeng, W. Y., Chen, C. K. M., Zhang, Y. H., Song, Y. C., Kuo, C. J., Yin, F. L., Oldfield, E., and Wang, A. H. J. (2007) Bisphosphonates target multiple sites in both *cis*- and *trans*-prenyltransferases. *Proc. Natl. Acad. Sci. U. S. A. 104*, 10022−10027.

(11) Tarshis, L. C., Yan, M. J., Poulter, C. D., and Sacchettini, J. C. (1994) Crystal structure of recombinant farnesyl diphosphate synthase at 2.6-Angstrom resolution. *Biochemistry 33*, 10871−10877.

(12) Guo, R. T., Kuo, C. J., Chou, C. C., Ko, T. P., Shr, H. L., Liang, P. H., and Wang, A. H. J. (2004) Crystal structure of octaprenyl pyrophosphate synthase from hyperthermophilic *Thermotoga maritima* and mechanism of product chain length determination. *J. Biol. Chem. 279*, 4903−4912.

(13) Hosfield, D. J., Zhang, Y. M., Dougan, D. R., Broun, A., Tari, L. W., Swanson, R. V., and Finn, J. (2004) Structural basis for bisphosphonate-mediated inhibition of isoprenoid biosynthesis. *J. Biol. Chem. 279*, 8526−8529.

(14) Sun, H. Y., Ko, T. P., Kuo, C. J., Guo, R. T., Chou, C. C., Liang, P. H., and Wang, A. H. J. (2005) Homodimeric hexaprenyl pyrophosphate synthase from the thermo acidophilic crenarchaeon Sulfolobus solfataricus displays asymmetric subunit structures. *J. Bacteriol. 187*, 8137−8148.
(15) Gabelli, S. B., McLellan, J. S., Montalvetti, A., Oldfield, E., Docampo, R., and Amzel, L. M. (2006) Structure and mechanism of the farnesyl diphosphate synthase from *Trypanosoma cruza*: Implications for drug design. *Proteins: Struct., Funct., Bioinf. 62*, 80−88.
(16) Chang, T. H., Guo, R. T., Ko, T. P., Wang, A. H. J., and Liang, P. H. (2006) Crystal structure of type-III geranylgeranyl pyrophosphate synthase from *Saccharomyces cerevisiae* and the mechanism of product chain length determination. *J. Biol. Chem. 281*, 14991−15000.
(17) Kavanagh, K. L., Dunford, J. E., Bunkoczi, G., Russell, R. G. G., and Oppermann, U. (2006) The crystal structure of human geranylgeranyl pyrophosphate synthase reveals a novel hexameric arrangement and inhibitory product binding. *J. Biol. Chem. 281*, 22004−22012.
(18) Kloer, D. P., Welsch, R., Beyer, P., and Schulz, G. E. (2006) Structure and reaction geometry of geranylgeranyl diphosphate synthase from *Sinapis alba*. *Biochemistry 45*, 15197−15204.
(19) Lo, C. H., Chang, Y. H., Wright, J. D., Chen, S. H., Kan, D., Lim, C., and Liang, P. H. (2009) Combined experimental and theoretical study of long-range interactions modulating dimerization and activity of yeast geranylgeranyl diphosphate synthase. *J. Am. Chem. Soc. 131*, 4051−4062.
(20) De Clercq, E. (2002) Strategies in the design of antiviral drugs. *Nat. Rev. Drug Discovery 1*, 13−25.
(21) Morriset, Jd, David, J. S. K., Pownall, H. J., and Gotto, A. M. (1973) Interaction of an Apolipoprotein (Apolp-Alanine) with Phosphatidylcholine. *Biochemistry 12*, 1290−1299.
(22) Chen, A. J., Kroon, P. A., and Poulter, C. D. (1994) Isoprenyl diphosphate synthases - Protein-sequence comparisons, a phylogenetic tree, and predictions of secondary structure. *Protein Sci. 3*, 600−607.
(23) Chang, K. M., Chen, S. H., Kuo, C. J., Chang, C. K., Guo, R. T., Yang, J. M., and Liang, P. H. (2012) Roles of amino acids in the *Escherichia coli* octaprenyl diphosphate synthase active site probed by structure-guided site-directed mutagenesis. *Biochemistry 51*, 3412−3419.